

# Homotopy Perturbation Method for Mathematical Modeling of Listeriosis and Anthrax Diseases

S. Rekha<sup>1</sup>, P. Balaganesan<sup>1</sup>, J. Renuka<sup>2</sup>

<sup>1</sup>*Department of Mathematics, AMET Deemed to be University,  
Chennai – 603112, Tamil Nadu, India.*

<sup>2</sup>*Department of Mathematics, women's Christian College,  
Chennai – 600006, Tamil Nadu, India.*

**Abstract:** Listeriosis and Anthrax are fatal zoonotic diseases caused by *Listeria monocytogene* and *Bacillus Anthracis*, respectively. In this paper, the mathematical Modeling of Listeriosis and Anthrax diseases is analysed. The mathematical modelling of Listeriosis and Anthrax is formulated into first order system of linear differential Equations and first order nonlinear differential Equations, respectively. The analytical solutions of both model is approached by the Homotopy Perturbation Method (HPM) and also simulation results are found. Finally, the analytical solutions, simulation results are compared and satisfactory agreement is noted.

**Keywords:** Homotopy Perturbation Method, Listeriosis Model, Anthrax Model, System of First Order Linear and Nonlinear Differential Equations.

## 1. Introduction

The development of numerical techniques for solving system of linear and nonlinear differential equations is a subject of considerable interest. There are many papers that deals with linear and nonlinear differential equations. The application of Homotopy Perturbation Method in linear and nonlinear problems has been adopted by researchers, because this method is to continuously deform a simple problem. This method, Homotopy Perturbation Method (HPM) was first propose by J. H. He [1].

Listeriosis and Anthrax are deadly zoonotic diseases, caused respectively by *Listeria monocytogene* and *Bacillus Anthracis*. In infants listeriosis can be acquired in two forms. This is usually contracted by mothers after consuming foods infected with *Listeria monocytogee*, and

may cause sepsis that results in chorioamnionitis and delivers a septic baby or fetus. In addition, mothers in the gastrointestinal tract who carry pathogens that infects their babies skin and respiratory tract during childbirth. *Listeria monocytogenes* are among the most dangerous pathogens that are responsible for neonatal bacterial meningitis.

Responsible factors for the disease include mediated HIV-related immune suppression, hemochromatosis of hematologic malignancies, cirrhosis, diabetes and hemodialysis renal failure [4]. Author in [5] developed a model for transmission of Anthrax, but never considered transmission in either animal or human populations. Our model is an enhancement of the author's research done in [5,6]. Both proposed models of Anthrax but focused only on the spread of the disease in the cases of animals. Anthrax disease is caused by infections of the bacteria and affects both humans and animals.

Our model is an improvement of the two models as we found Anthrax a zoonotic disease and also looked at the sensitivity analysis and the impact of the contact rate on the transmission of disease. A paper on the efficacy of constant and pulse vaccination policies using the SIR model was published by the authors in [7]. Analysis of their findings under constant vaccination has shown that the disease model dynamics are close to dynamics without vaccination [8 , 9]. There are some results about the spread of zoonotic diseases, but a majority of these studies concentrate on the impact of vaccination on disease distribution and transmission as in the case of authors in [10]. In addition, the authors in [11] explored a model for disease transmission by considering the effect of preventive vaccine and established the optimal threshold for vaccine coverage needed for disease eradication. However, the authors in [12] used optimal control to test with a vaccine strategy a nonlinear SIR disease model. Using the SIR epidemic model [13 - 15], several mathematical modeling techniques were used to research the function of optimal control. In [16], the authors proposed an outbreak model for SIR by considering vaccination as a control factors in their model.

Authors in [17] developed a statistical model for the dynamics of Listeriosis transmission in animal and human populations but did not use optimal control as a control measure to fight the disease. With the introduction of the vaccine compartment they divided the animal population into four compartment they divided the animal population into four compartment. Authors in [18] developed a model and used a optimal control to investigate the effect of chemotherapy on immigrant - infected malaria and [19] applied optimal control method relevant

to the prevention of exogenous reinfection based on exogenous tuberculosis model. Author in [20], performed work on on pathogen recognition and reservoirs to effectively monitor infectious disease and epidemics. *Listeria monocytogenes* is one of the main zoonotic foodborne pathogen that annually accounts for around twenty-eight percent of the majority food related death in the United States and is a significant cause of severe product recalls worldwide. A possible source and reservoir of *Listeria monocytogenes* has been found at the dairy farm. Models are commonly used in the study of the infectious disease transmission dynamics. In recent time the use of mathematical models has increased tremendously in the study of infectious disease. Then a branch called mathematical epidemiology emerges. Frequent diagnostic studies, clinical data availability and electronic monitoring have encouraged the development of mathematical models for critical analysis of scientific theories and for the implementation of real-life disease prevention strategies [21,22]. Authors in [23] developed a malaria and cholera co-infection model. Analysis of susceptibility defines the most important parameters for the model, and the analysis of infection force defines the effect of the contact rate on the transmission of disease.

## 2.1 Listeriosis Model Description and Formula

In this section [27], the model divides the total human and vector population at any time 't' into five components with respect to disease status in the system. The total population is represented by  $\Omega_h$ . It is divided into components of Susceptible humans ( $S_h$ ), Infectious vector ( $I_v$ ) and Recovered vector ( $R_v$ ), which implies  $N_h(t) = S_h(t) + I_v(t) + R_v(t)$ . The susceptible humans are recruited into the population at a rate  $\mu_h$ . Individuals recover from the disease at a rate of  $\delta$ . Humans who are infected with listeriosis die at a rate 'm' and the recovered humans may lose immunity and return to the susceptible component at a rate  $\omega$ . The natural death rate of the entire human's component is  $\mu_h$ . The vector population is represented by  $C_p$ . But  $C_p$  is connected with  $\pi = \gamma C_p / (C_p + k)$ . The concentration of carcasses and ingestion rate are denoted by K and  $\gamma$  respectively. Let  $\rho$  and  $\mu_b$  are denote the listeriosis contribution to environment and bacteria death rate respectively. The below figure 1 [27] is the flow chart of Listeriosis model.

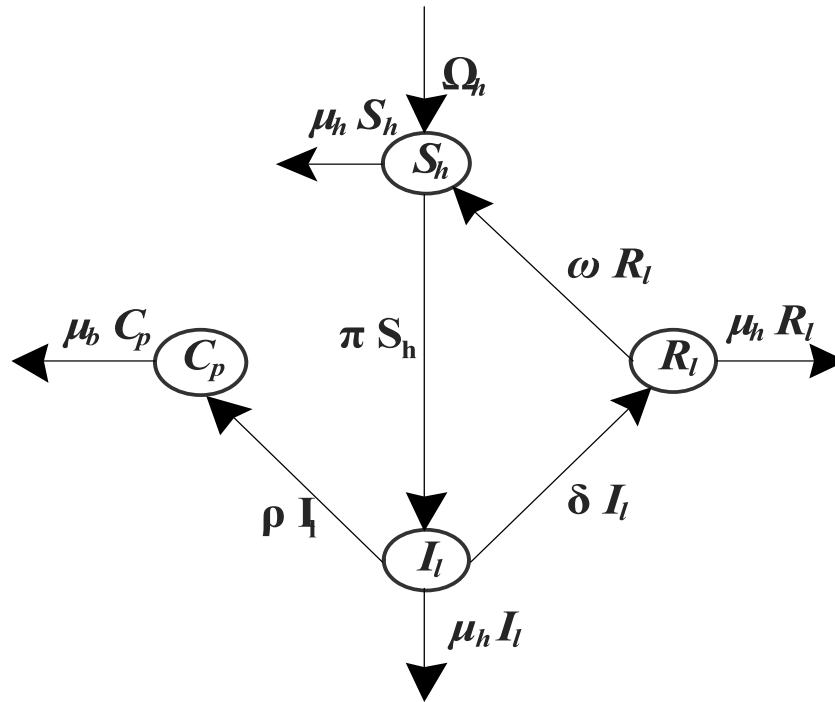


**Figure 1: Flow Chart of Listeriosis Model**

## 2.2 Analysis of Listeriosis Model

In this section [27], Listeriosis model is considered in the analysis of the transmission dynamics.

$$\frac{dS_h}{dt} = \Omega_h + \omega R_l - \pi S_h - \mu_h S_h \quad (1)$$

$$\frac{dI_l}{dt} = \pi S_h - (\delta + \mu_h + m) I_l \quad (2)$$

$$\frac{dR_l}{dt} = \delta I_l - (\omega + \mu_h) R_l \quad (3)$$

$$\frac{dC_p}{dt} = \rho I_l - \mu_b C_p \quad (4)$$

Where,  $\Omega_h = 0.001$ ,  $\omega = 0.001$ ,  $\pi = 0.5$ ,  $\mu_h = 0.2$ ,  $\delta = 0.002$ ,  $m = 0.2$ ,  $\rho = 0.65$ ,  $\mu_b = 0.0025$ .

With the initial condition,  $\left(\frac{dS_h}{dt}, \frac{dI_l}{dt}, \frac{dR_l}{dt}, \frac{dC_p}{dt}\right) = \left(\frac{\Omega_h}{\mu_h}, 0, 0, 0\right)$  when  $t = 0$ ,

The analytical solution is obtained by Homotopy Perturbation Method,

$$S_h(t) = 0.003572e^{(-0.7t)} + 0.0014286 \quad (5)$$

$$I_l(t) = 0.001776 - 0.00599e^{(-0.7t)} + 0.0042172e^{(-0.402t)} \quad (6)$$

$$R_l(t) = 0.0000177 - 0.0000419e^{(-0.402t)} + 0.0000241e^{(-0.7t)} + 0.0000027e^{(-0.201t)} \quad (7)$$

$$C_p(t) = 0.46176 - 0.006866e^{(-0.402t)} + 0.005592e^{(-0.7t)} - 0.4605e^{(-0.0025t)} \quad (8)$$

### 2.3 Numerical Simulation for Listeriosis Model

In this model, numerical solution is found by MATLAB programming, and it is compared with analytical solution for various parameters in table 1. For this study, we used the parameters values in table 1 were referred in [27]. The following figures illustrate the simulation showing the comparison of the analytical solution and numerical solution for various values the parameters.

Parameters	Description	Value
$\emptyset$	Anthrax related death rate	0.2
$\beta_h$	Human transmission rate	0.01
M	Listeriosis related death rate	0.2
$\beta_v$	Vector transmission rate	0.05
K	Anthrax waning immunity	0.02
$\mu_v$	Vector natural death rate	0.0004
$\Omega_v$	Vector recruitment rate	0.005
$\Omega_h$	Human recruitment rate	0.001
$\delta$	Listeriosis recovery rate	0.002
$\alpha$	Anthrax recovery rate	0.33
$\rho$	Listeriosis contribution to environment	0.65
$\mu_h$	Human natural death rate	0.2
$\mu_b$	Bacterial death rate	0.0025
$\omega$	Listeriosis waning immunity	0.001
$\pi$	Concentration of carcasses	0.5

**Table 1: Variable and Parameter values of the coinfection model**

### $S_h$ - Susceptible humans:

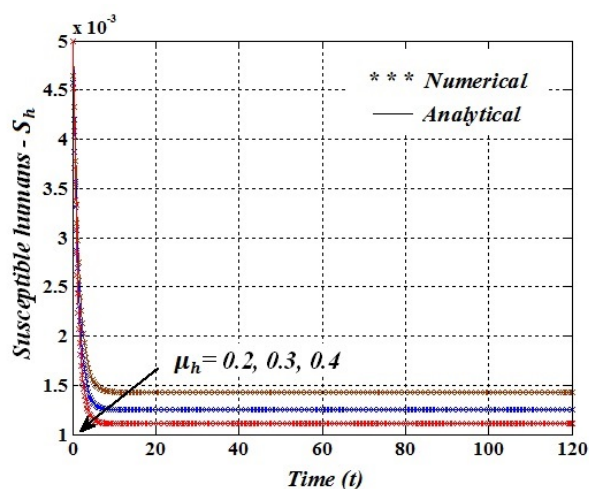


Figure 2: Simulation showing the decreasing effect of infection on susceptible humans of Listeriosis disease for various values of  $\mu_h$

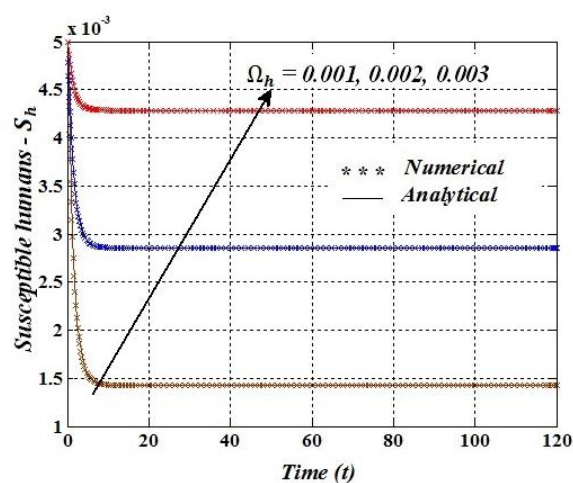


Figure 3: Simulation showing the increasing effect of infection on susceptible humans of Listeriosis disease for various values of  $\Omega_h$

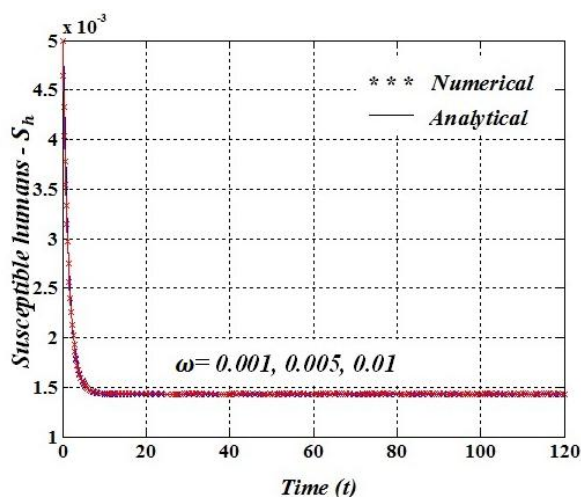


Figure 4: Simulation showing the effect of infection on susceptible humans of Listeriosis disease for various values of  $\omega$

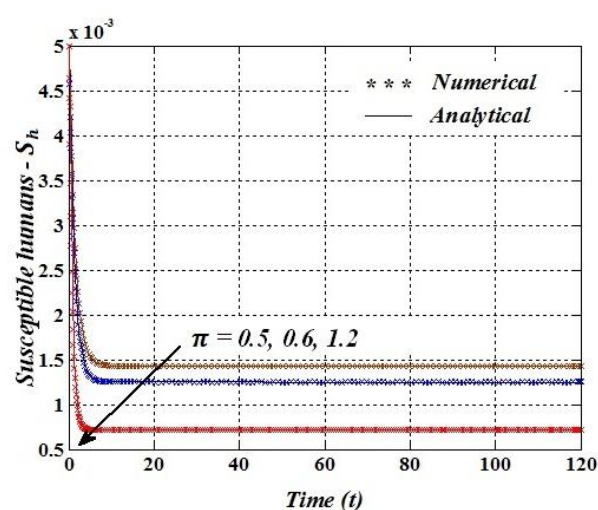
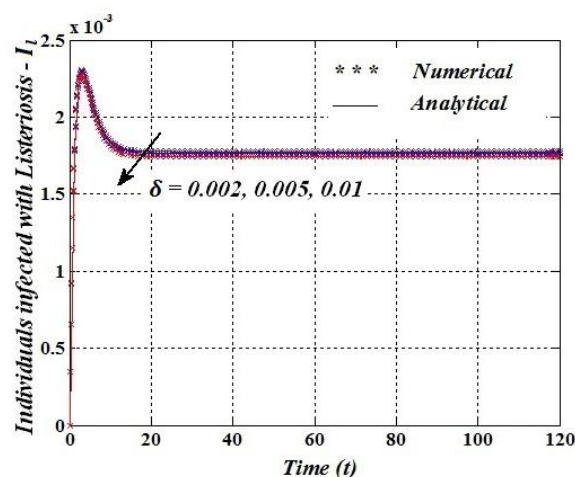
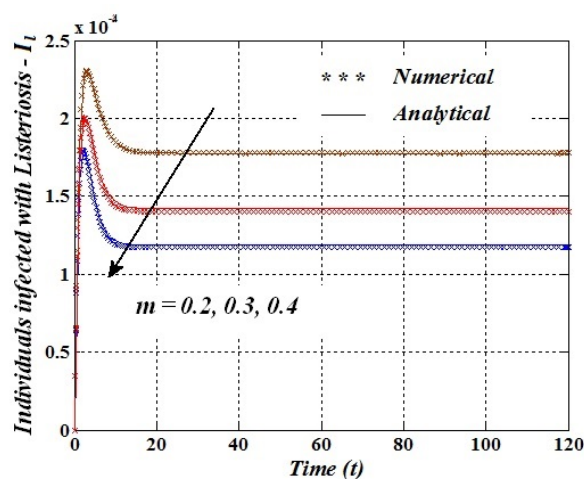


Figure 5: Simulation showing the decreasing effect of infection on susceptible humans of Listeriosis disease for various values of  $\pi$

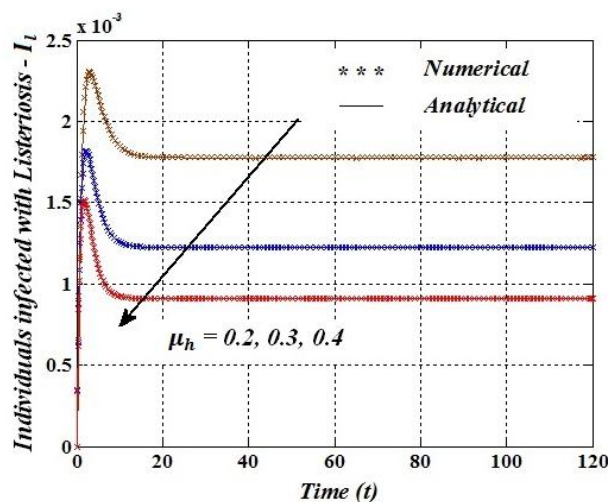
### $I_I$ - Individuals infected with Listeriosis:



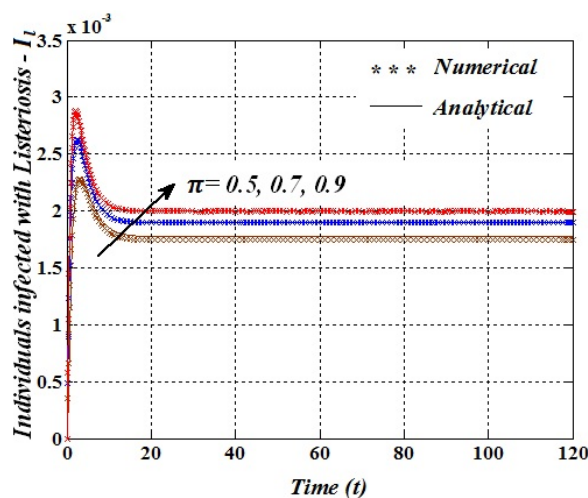
**Figure 6:** Simulation showing the decreasing effect of infection on individuals of Listeriosis disease for various values of  $\delta$



**Figure 7:** Simulation showing the decreasing effect of infection on individuals of Listeriosis disease of various values of  $m$

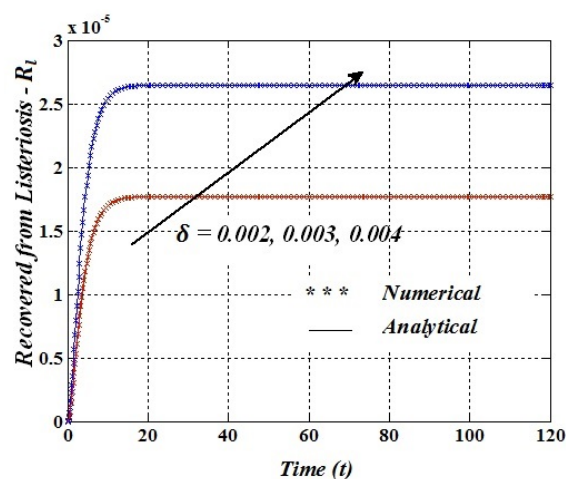


**Figure 8:** Simulation showing the decreasing effect of infection on individuals of Listeriosis disease for various values of  $\mu_h$

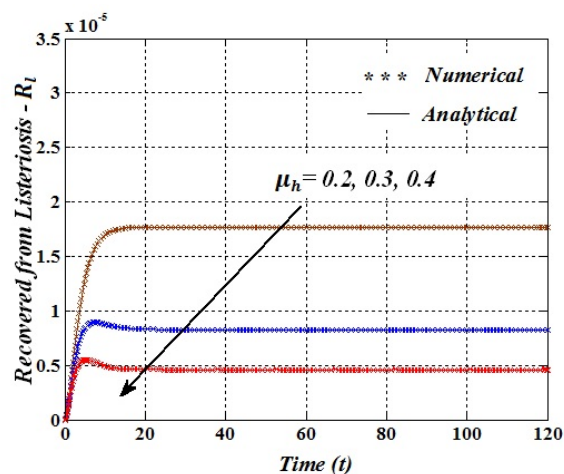


**Figure 9:** Simulation showing the increasing effect of infection on individuals of Listeriosis disease of various values of  $\pi$

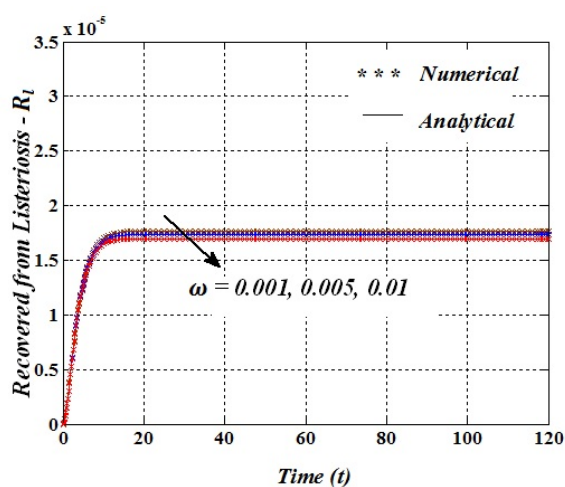
### $R_I$ - Recovered from Listeriosis:



**Figure 10: Simulation showing the increasing effect of infection on recovered humans of Listeriosis disease for various values of  $\delta$**

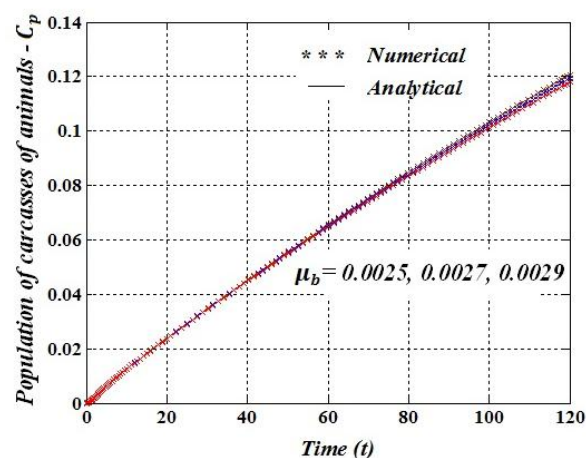


**Figure 11: Simulation showing the decreasing effect of infection on recovered humans of Listeriosis disease for various values of  $\mu_h$**



**Figure 12: Simulation showing the decreasing effect of infection on recovered humans of Listeriosis disease for various values of  $\omega$**



**$C_p$  - Population of Carcasses of Animals:**

**Figure 13: Simulation showing the effect of infection on carcasses of animals of Listeriosis disease for various values of  $\mu_b$**

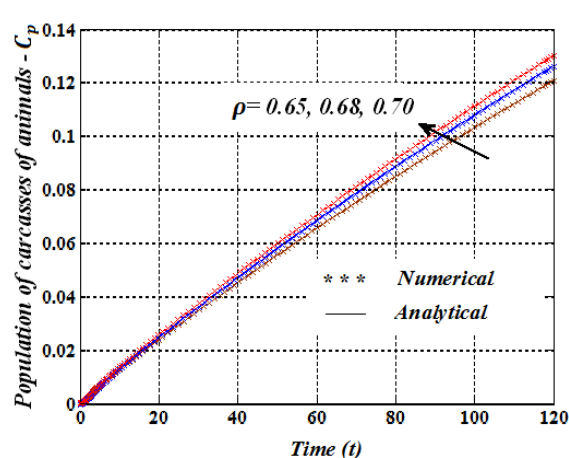


**Figure 14: Simulation showing the increasing effect of infection on carcasses of animals of Listeriosis disease for various values of  $\rho$**

### 3.1 Anthrax Model Description and Formulation

In this section [27], the model divides the total human and vector population at any time ' $t$ ' into five components with respect to disease status in the system. The total human population is represented by  $\Omega_h$ . It is divided into components of Susceptible humans ( $S_h$ ), individuals infectious vector ( $I_a$ ) and individuals recovered vector ( $R_a$ ), which implies  $N_h(t) = S_h(t) + I_a(t) + R_a(t)$ . The total vector population represented by  $N_v$ ; this is divided into sub components that consists of susceptible animals  $S_v$  and animals infected with anthrax  $I_v$ ; which implies  $N_v(t) = S_v(t) + I_v(t)$ . The total vector population is represented by  $\Omega_v$ . The human transmission rate  $\beta_h$ , Anthrax waning immunity  $k$ , anthrax recovery rate  $\alpha$ , anthrax related death rate  $\phi$ ,  $\beta_v$ ,  $\mu_v$ , are denoted the vector transmission rate and vector natural death rate respectively. The natural death rate of the entire human's component is  $\mu_h$ . The below figure 2 [27] is the flow chart of Anthrax model.

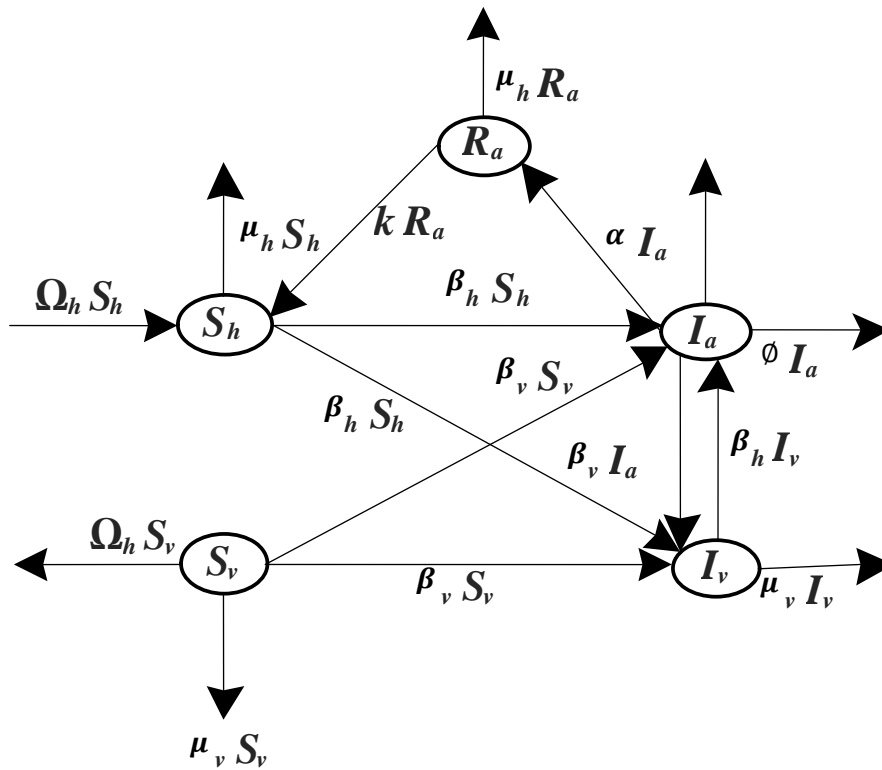


**Figure 15** Flow Chart of Anthrax Model

### Analysis of Anthrax Model:

In this section, Anthrax model is considered in the analysis of the transmission dynamics.

$$\frac{dS_h}{dt} = \Omega_h + kR_a - \beta_h S_h I_v - \mu_h S_h \quad (9)$$

$$\frac{dI_a}{dt} = \beta_h S_h I_v - (\alpha + \mu_h + \phi) I_a \quad (10)$$

$$\frac{dR_a}{dt} = \alpha I_a - (k + \mu_h) R_a \quad (11)$$

$$\frac{dS_v}{dt} = \Omega_v - \beta_v S_v I_a - \mu_v S_v \quad (12)$$

$$\frac{dI_v}{dt} = \beta_v S_v I_a - \mu_v I_v \quad (13)$$

Where,  $\Omega_h = 0.001$ ,  $k = 0.02$ ,  $\beta_h = 0.01$ ,  $\mu_h = 0.2$ ,  $\alpha = 0.33$ ,  $\phi = 0.2$ ,  $\Omega_v = 0.005$ ,  $\beta_v = 0.05$ ,

$\mu_v = 0.0004$ , With the initial condition,  $\left(\frac{dS_h}{dt}, \frac{dI_a}{dt}, \frac{dR_a}{dt}, \frac{dS_v}{dt}, \frac{dI_v}{dt}\right) = \left(\frac{\Omega_h}{\mu_h}, 0, 0, \frac{\Omega_v}{\mu_v}, 0\right)$ , when  $t = 0$ ,

The analytical solution is obtained by Homotopy Perturbation Method as follows:

$$S_h(t) = 0.005 - 4.8759e^{(-0.2t)} - 0.001647e^{(-0.22t)} - 0.0005e^{(-0.0004t)} + 9.8749e^{(-0.2004t)} - 0.00098e^{(-0.2204t)} + 0.000051e^{(-0.0008t)} - 5e^{(-0.2008t)} + 0.0000148e^{(-0.7304t)} \quad (14)$$

$$I_a(t) = 0.02071e^{(-0.73t)} + 0.000137e^{(-0.0004t)} + 0.00746e^{(-0.2004t)} - 0.000039e^{(-0.2204t)} - 0.0000137e^{(-0.0008t)} - 0.007558e^{(-0.2008t)} - 0.00000856e^{(-0.73t)}t - 0.1969e^{(-0.7304t)} \quad (15)$$

$$R_a(t) = 0.00399e^{(-0.22t)} - 0.00066e^{(-0.73t)} + 0.000206e^{(-0.0004t)} - 0.0025e^{(-0.2004t)} \quad (16)$$

$$S_v(t) = 12.500 - 11.500069e^{(-0.0004t)} + 0.000856e^{(-0.73t)} - 0.0007877e^{(-0.7304t)} \quad (17)$$

$$I_v(t) = 1.803005e^{(-0.0004t)} - 0.00087e^{(-0.73t)} + 0.00079e^{(-0.7304t)} + 0.0000856e^{(-0.0004t)}t + 0.00047e^{(-0.2004t)} + 0.1971e^{(-0.0008t)} - 0.0004e^{(-0.2008t)} \quad (18)$$

### 3.2 Numerical Simulation for Anthrax Model

In this model, it has been found that numerical solution by MAT programming, and it is compared with analytical solution for various parameters in table 1. For this study, we used the parameters values in table 1 were referred in [27]. The following figures illustrate the simulation showing the comparison of the analytical solution and numerical solution for various values the parameters.

**$S_h$  - Susceptible humans:**

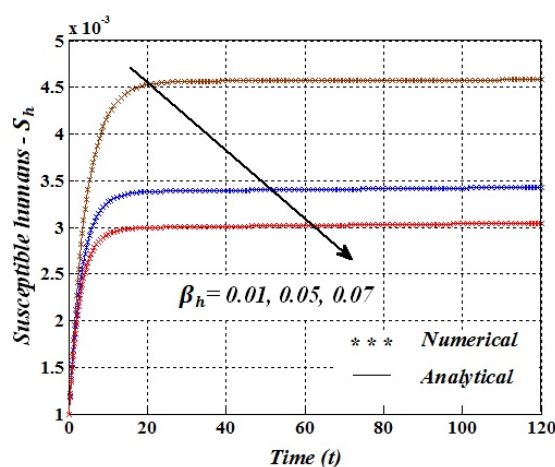


**Figure 16: Simulation showing the decreasing effect of infection on susceptible humans of**

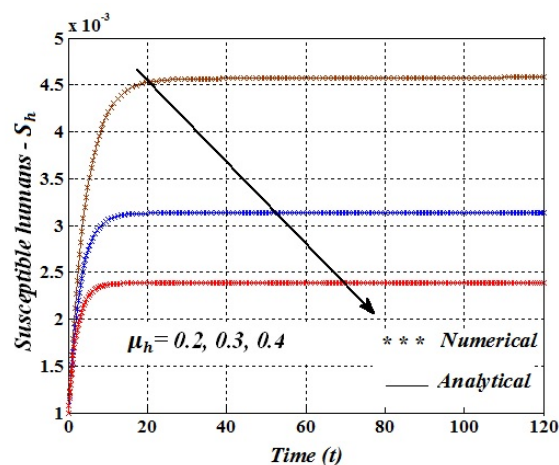


**Figure 17: Simulation showing the decreasing effect of infection on susceptible humans**

### of Anthrax disease of various values of $\beta_h$

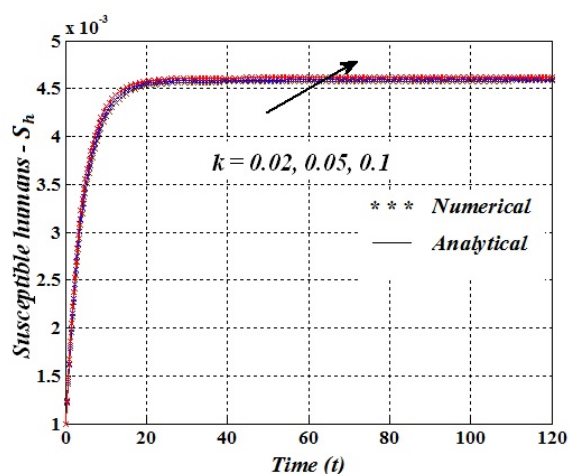


Figure 18: Simulation showing the increasing effect of infection on susceptible humans of Anthrax disease of various values of  $k$

### of Anthrax disease of various values of $\mu_h$

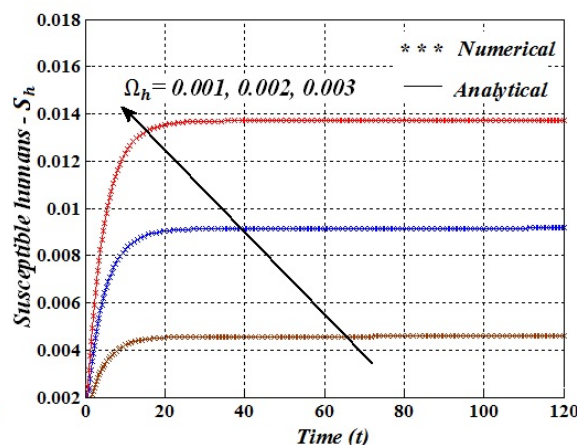


Figure 19: Simulation showing the increasing effect of infection on susceptible human of Anthrax disease of various values of  $\Omega_h$

### $I_a$ - Individuals infected with Anthrax:

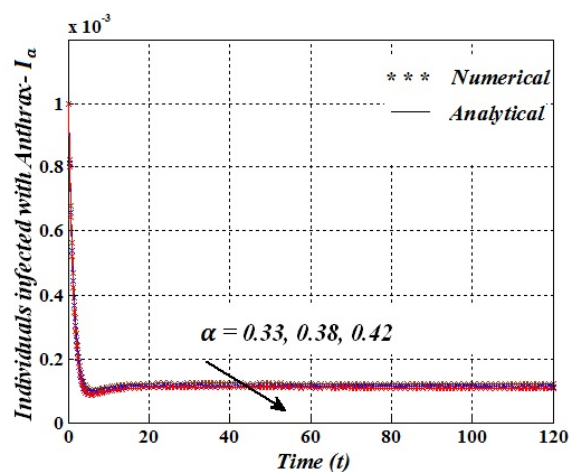


Figure 20: Simulation showing the decreasing effect of infection on individuals of Anthrax disease of various values of  $\alpha$

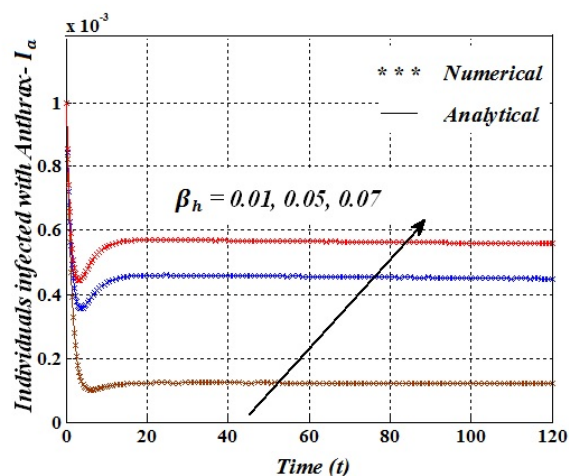


Figure 21: Simulation showing the increasing effect of infection on individuals of Anthrax disease of various values of  $\beta_h$

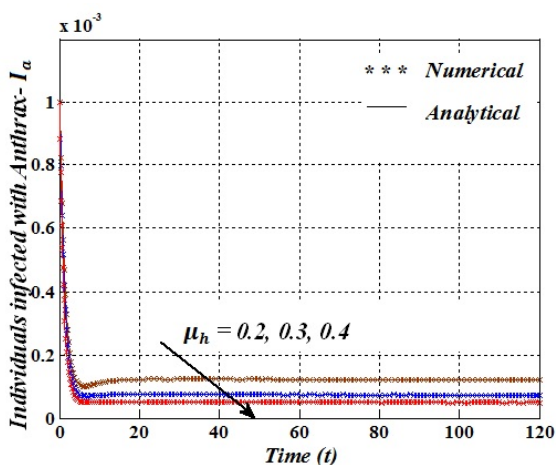


Figure 22: Simulation showing the decreasing effect of infection on individuals of Anthrax disease of various values of  $\mu_h$

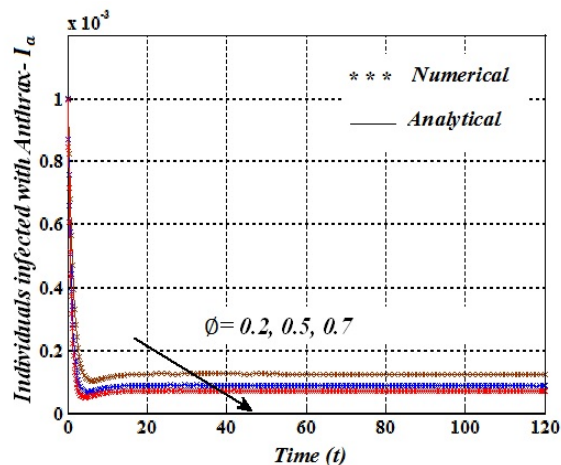


Figure 23: Simulation showing the decreasing effect of infection on individuals of Anthrax disease of various values of  $\phi$

#### $R_a$ - Recovered from Anthrax:

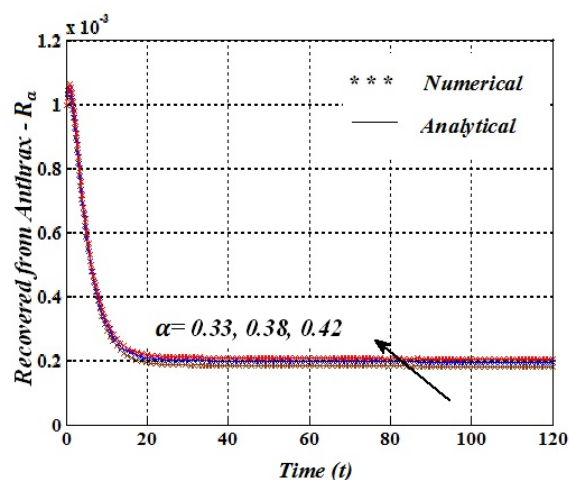


Figure 24: Simulation showing the increasing effect of infection on recovered humans of Anthrax disease of various values of  $\alpha$

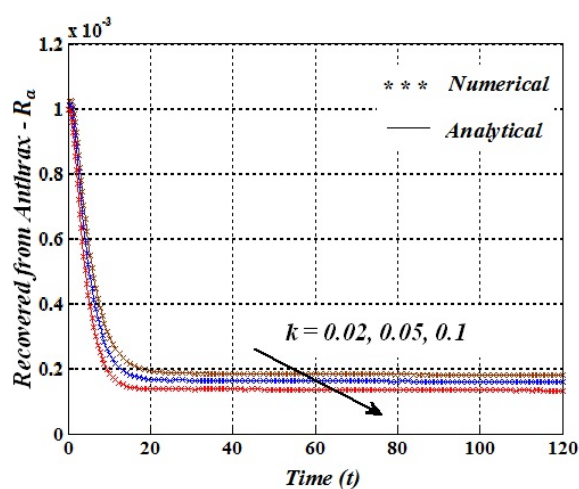
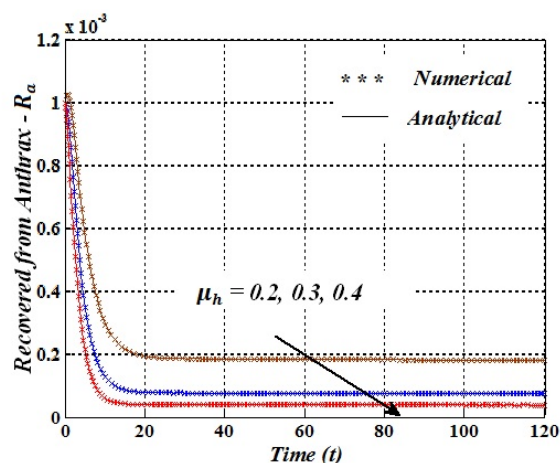
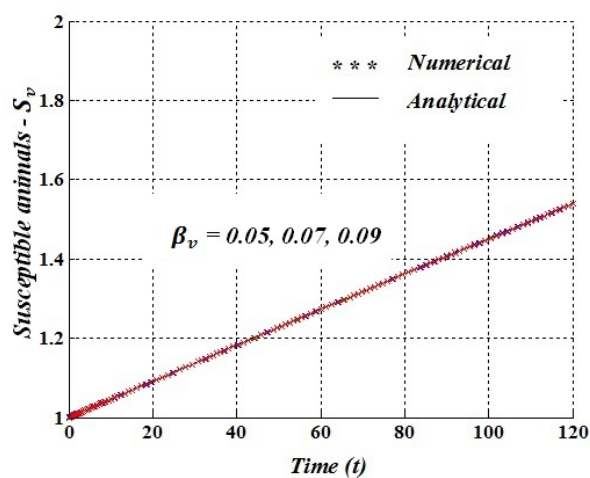


Figure 25: Simulation showing the decreasing effect of infection on recovered humans of Anthrax disease of various values of  $k$



**Figure 26: Simulation showing the decreasing effect of infection on recovered humans of Anthrax disease of various values of  $\mu_h$**

**$S_v$  - Susceptible Animals:**



**Figure 27: Simulation showing the effect of infection on susceptible animals of Anthrax disease of various values of  $\beta_v$**

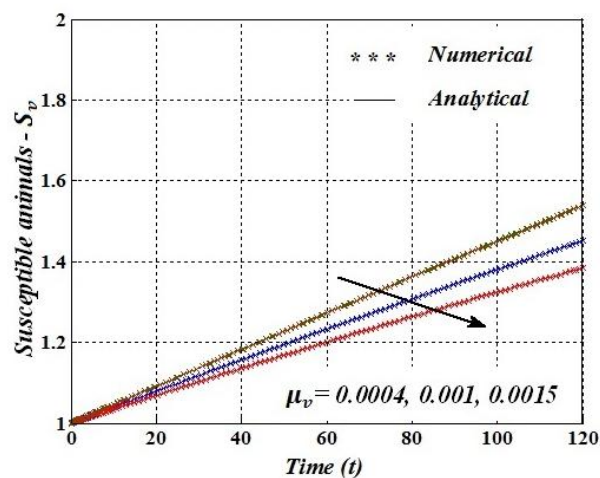


**Figure 28: Simulation showing the decreasing effect of infection on susceptible animals of Anthrax disease of various values of  $\mu_v$**



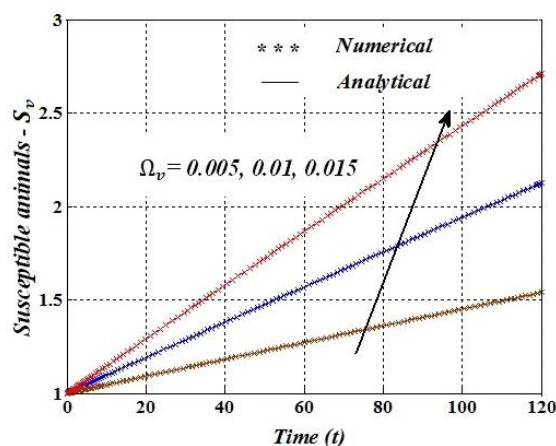


**Figure 29: Simulation showing the increasing effect of infection on susceptible animals of anthrax disease of various values of  $\Omega_v$**

**$I_v$  - Animals infected with Anthrax:**

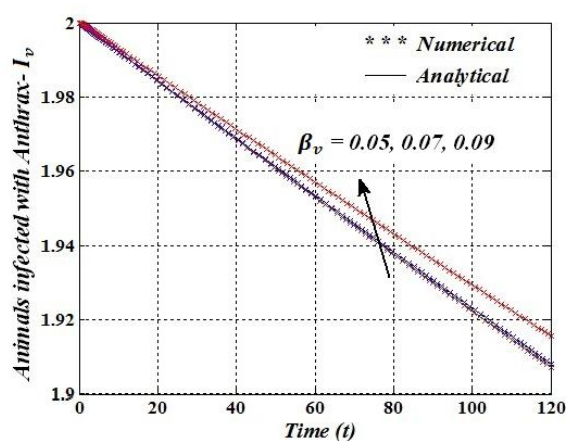


**Figure 30: Simulation showing the increasing effect of infection on animals of Anthrax disease of various values of  $\beta_v$**

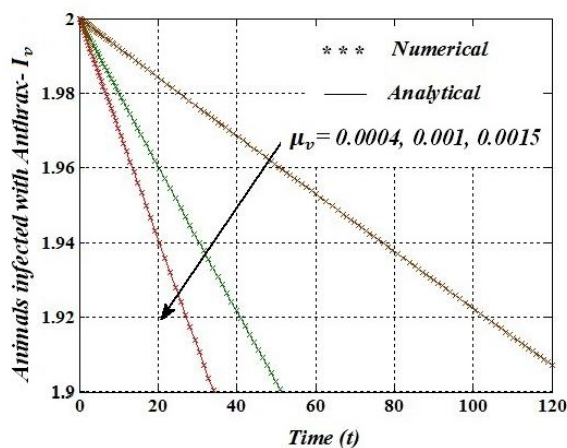


**Figure 31: Simulation showing the decreasing effect of infection on animals of Anthrax disease of various values of  $\mu_v$**

#### 4. Results and Discussions:

An analysis of listeriosis model consisting of four dependent variable  $S_h, I_b, R_b, C_p$  is made. Each of them has four, four, three and two parameters respectively. Depending upon the three different values of the parameters of the dependent variable, numerical and analytical solution of them are

obtained. A comparative study of the numerical solution and analytical solution so obtained shows that both the solution agrees to each other.

Figure 2-5 is Susceptible humans, Figure 2 and 5 showing the simulation of decreasing effect of infection on susceptible humans of Listeriosis disease for various values of  $\mu_h = 0.2, 0.3, 0.4$  and  $\pi = 0.5, 0.6, 1.2$ , Figure 3 showing the simulation of increasing effect of infection on Susceptible humans of Listeriosis disease for various values of  $\Omega_h = 0.001, 0.002, 0.003$ .

Figure 6-8, illustrates the decreasing effect of Individual infected  $I_l$  as time increases from various values of the population  $N_h(t)$ . Figure 9 shows the increasing effect of infection on individuals infected in Listeriosis disease of various values of  $\pi = 0.5, 0.7, 0.9$ , and Figure 10 determines the increasing effect of infection on Recovered humans in Listeriosis disease of various values of  $\delta = 0.002, 0.003, 0.004$ .

In Figure 11-12, x-axis and y-axis represent time 't'. The decreasing effect of infection on recovered humans of Listeriosis disease for various values of  $\mu_h = 0.2, 0.3, 0.4$  and  $\omega = 0.001, 0.005, 0.01$ . Population of Carcasses of animals illustrates the increasing effect of simulation result by increasing the values of  $\mu_b = 0.0025, 0.0027, 0.0029$  and  $\rho = 0.65, 0.68, 0.70$

An analysis of Anthrax model consisting of five dependent variable  $S_h, I_a, R_a, S_v, I_v$  is made. Each of them has four, four, three, three and two parameters respectively. Depending upon the three different values of the parameters of the dependent variable, numerical and analytical solution of them are obtained. A comparative study of the numerical solution and analytical solution so obtained shows that both the solution agrees to each other.

In Figure 16-17, simulation showing the decreasing effect of infection on Susceptible humans of Anthrax disease of various values of  $\beta_h = 0.01, 0.05, 0.07$  and  $\mu_h = 0.2, 0.3, 0.4$  and in Figure 18-19, shows the increasing effect of infection on susceptible humans of Anthrax disease of various values of  $k = 0.02, 0.05, 0.1$  and  $\Omega_h = 0.001, 0.002, 0.003$ .



Figure 20, 22 and 23, illustrates the decreasing effect of infection on individuals of Anthrax disease by increasing the values of parameters  $\alpha = 0.33, 0.38 \text{ and } 0.42$ ,  $\mu_h = 0.2, 0.3, 0.4$  and  $\phi = 0.2, 0.5, 0.7$

$R_a$  is the Recovered humans from Anthrax in figure 24, that illustrates the simulation of increasing effect of infection on recovered humans of Anthrax disease of various values of  $\alpha = 0.33, 0.38, 0.42$  and in Figure 25, 26 shows the decreasing effect of infection on recovered humans of Anthrax disease of various values of  $k = 0.02, 0.05, 0.1$  and  $\mu_h = 0.2, 0.3, 0.4$ .

In figure 27, Vector transmission rate has no changes in simulation by changing the parameter values of  $\beta_v = 0.05, 0.07, 0.09$  and then in figure 28, 29 the simulation decreased and increased in the effect of infection on Susceptible animals of Anthrax for various values of  $\mu_v = 0.0004, 0.001, 0.0015$  and  $\Omega_v = 0.005, 0.01, 0.015$ .

Animals infected with Anthrax  $I_v$  shows the simulation of increasing and decreasing effect in Figure 30 and 31, infection on animals of Anthrax disease of various values of  $\beta_v = 0.05, 0.07, 0.09$  and  $\mu_v = 0.0004, 0.001, 0.0015$ .

## 5. Conclusion:

In this paper, the mathematical Modeling of Listeriosis and Anthrax diseases is analysed. The mathematical modeling of Listeriosis and Anthrax is formulated into first order system of linear differential Equations and first order nonlinear differential Equations, respectively. The analytical solutions of both model is approached by the Homotopy Perturbation Method (HPM) and also found simulation results are also found. Finally, the analytical solutions, simulation results are compared and satisfactory agreement is noted.

**Acknowledgments:** The authors are also thankful to Shri J. Ramachandran, Chancellor, Col. and Dr.G.Thiruvasagam, Vice-Chancellor, Academy of Maritime Education and Training (AMET), Chennai, Tamil Nadu.

**Ethical Clearance:** Taken from AMET University, Chennai.

**Source of funding:** Self

**Conflict of interest:** Nil

**Data Availability:**

The data supporting this deterministic model are taken from previously published articles and they have been duly cited in this paper. Those parameter values taken from published articles are cited in Table 1 of this paper. These published articles are also cited at relevant places within the text as reference.

## References:

- [1] J.H. He, Homotopy perturbation technique, *Comp. Meth. Appl. Mech. Eng.* 178 (1999) 257 - 262.
- [2] J.H. He, A coupling method of homotopy technique and a perturbation technique for non linear problems, *Int.J. Non linear Mech.* 35 (2000) 37-43.
- [3] J.H. He, Homotopy perturbation method: A new nonlinear analytical technique, *Appl. Math. Comput.* 135 (2003) 73-79.
- [4] W. F. Schlech and D. Acheson, "Foodborne listeriosis," *Clinical Infectious Diseases*, vol. 31, no. 3, pp. 770–775, 2000.
- [5] C. M. Saad-Roy, P. van den Driessche, and A.-A. Yakubu, "A mathematical model of anthrax transmission in animal populations," *Bulletin of Mathematical Biology*, vol. 79, no. 2, pp. 303–324, 2017.
- [6] A. Friedman and A. A. Yakubu, "Anthrax epizootic and migration: persistence or extinction," *Mathematical Biosciences*, vol. 241, no. 1, pp. 137–144, 2013.
- [7] Z. Lu, X. Chi, and L. Chen, "The effect of constant and pulse vaccination on SIR epidemic model with horizontal and vertical transmission," *Mathematical and Computer Modelling*, vol. 36, no. 9-10, pp. 1039–1057, 2002.
- [8] A.A. Lashari and G. Zaman, "Optimal control of a vector borne disease with horizontal transmission," *Nonlinear Analysis: Real World Applications*, vol. 13, no. 1, pp. 203–212, 2012.
- [9] A. A. Lashari, "Optimal control of an SIR epidemic model with a saturated treatment," *Applied Mathematics & Information Sciences*, vol. 10, no. 1, pp. 185–191, 2016.
- [10] S. Mushayabasa and C. P. Bhunu, "Is HIV infection associated with an increased risk for cholera? Insights from a mathematical model," *BioSystems*, vol. 109, no. 2, pp. 203–213, 2012.
- [11] A. B. Gumel and S.M. Moghadas, "A qualitative study of a vaccination model with non-linear incidence," *Applied Mathematics and Computation*, vol. 143, no. 2-3, pp. 409–419, 2003.
- [12] T.K. Kar and A. Batabyal, "Stability analysis and optimal control of an SIR epidemic model with vaccination," *BioSystems*, vol. 104, no. 2-3, pp. 127–135, 2011.
- [13] O. D. Makinde, "Adomian decomposition approach to a SIR epidemic model with constant vaccination strategy," *Applied Mathematics and Computation*, vol. 184, no. 2, pp. 842–848, 2007.
- [14] T. T. Yusuf and F. Benyah, "Optimal control of vaccination and treatment for an SIR epidemiological model," *World Journal of Modelling and Simulation*, vol. 8, no. 3, pp. 194–204, 2012.
- [15] G. Zaman, Y. H. Kang, and I. H. Jung, "Optimal treatment of an SIR epidemic model with time delay," *BioSystems*, vol. 98, no. 1, pp. 43–50, 2009.

- [16] G. Zaman, Y. Han Kang, and I. H. Jung, "Stability analysis and optimal vaccination of an SIR epidemic model," *BioSystems*, vol. 93, no. 3, pp. 240–249, 2008.
- [17] O. Shaibu, D. M. Oluwole, and M. T. David, "Stability analysis and modelling of listeriosis dynamics in human and animal populations," *The Global Journal of Pure and Applied Mathematics (GJPAM)*, vol. 14, no. 1, pp. 115–137, 2018.
- [18] O. D. Makinde and K. O. Okosun, "Impact of chemo-therapy on optimal control of malaria disease with infected immigrants," *BioSystems*, vol. 104, no. 1, pp. 32–41, 2011.
- [19] K. Hattaf, M. Rachik, S. Saadi, Y. Tabit, and N. Yousfi, "Optimal control of tuberculosis with exogenous reinfection," *Applied Mathematical Sciences*, vol. 3, no. 5-8, pp. 231–240, 2009.
- [20] M. K. Borucki, J. Reynolds, C. C. Gay et al., "Dairy farm reservoir of *Listeria monocytogenes* sporadic and epidemic strains," *Journal of Food Protection*, vol. 67, no. 11, pp. 2496–2499, 2004.
- [21] H. W. Hethcote, "Qualitative analyses of communicable disease models," *Mathematical Biosciences*, vol. 28, no. 3-4, pp. 335–356, 1976.
- [22] N. C. Grassly and C. Fraser, "Mathematical models of infectious disease transmission," *Nature Reviews Microbiology*, vol. 6, no. 6, pp. 477–487, 2008.
- [23] K. O. Okosun and O. D. Makinde, "A co-infection model of malaria and cholera diseases with optimal control," *Mathematical Biosciences*, vol. 258, pp. 19–32, 2014.
- [24] L. Rajendran, S. Anitha, Reply to "Comments on analytical solution of amperometric enzymatic reaction based on Homotopy perturbation method," by Ji-Huan He, Lu-Feng Mo [Electrochim. Acta (2013)], *Electrochimica Acta* 102(2013)474 - 476.
- [25] K. Saranya, V. Mohan, R. Kizek, C. Fernandez, L. Rajendran, Unprecedented homotopy perturbation method for solving nonlinear equations in the enzymatic reaction of glucose in a spherical matrix, *Bioprocess and Biosystems Engineering*, 41(2), (2018), 281-294.
- [26] L. Rajendran, G. Rahamathunissa, The Application of He's variational iteration method to nonlinear boundary value problems in enzyme-substrate reaction diffusion processes : Part 1. The steady-state amperometric response, *Journal of Mathematical Chemistry* 44 (2008) 849-861.
- [27] Shaibu Osman and Oluwole Daniel Makinde, A Mathematical Model for Coinfection of Listeriosis and Anthrax Disease, *International Journal of Mathematics and Mathematical Science*, vol. 2018, article id 1725671.

## Appendix A: Basic concept of homotopy perturbation method (HPM)

To illustrate the basic ideas of this method, we consider the following nonlinear functional equation:

$$A(U) - f(r) = 0, \quad r \in \Omega \quad (\text{A1})$$

With the following boundary condition:

$$B\left(u, \frac{\partial u}{\partial n}\right) = 0, \quad r \in \Gamma, \quad (\text{A2})$$

where  $A$  is a general functional operator,  $B$  a boundary operator,  $f(r)$  is a known analytical function and  $\Gamma$  is the boundary of the domain  $\Omega$ . The operator  $A$  can be decomposed into two operators  $L$  and  $N$ , where  $L$  is linear, and  $N$  is nonlinear operator.

Eqn. (19) can be, therefore, written as follows:

$$L(U) + N(U) - f(r) = 0. \quad (A3)$$

Using the homotopy technique, we construct a homotopy  $U(r, p): \Omega \times [0, 1] \rightarrow R$ , which satisfies:

$$H(U, p) = (1-p)[L(U) - L(U_0)] + p[A(U) - f(r)] = 0, \quad p \in [0, 1], \quad r \in \Omega, \quad (A4)$$

or

$$H(U, p) = L(U) - L(U_0) + p[L(U_0) + p[N(U) - f(r)]] = 0, \quad (A5)$$

where  $p \in [0, 1]$  is an embedding parameter,  $u_0$  is an initial approximation for the solution of Eqn. (SA2), which satisfies the boundary conditions. Obviously, from Eqns. (A4) and (A5) we will have:

$$H(U, 0) = L(U) - L(U_0) = 0, \quad (A6)$$

$$H(U, 1) = A(U) - f(r) = 0. \quad (A7)$$

The changing values of  $p$  from zero to unity are just that of  $U(r, p)$  from  $u_0(r)$  to  $u(r)$ . In topology, this is called homotopy. According to HPM, we can first use the embedding parameter  $p$  as a small parameter and assume that the solution of Eqns. (A4) and (S5) as a power series in  $p$ :

$$V = U_0 + pU_1 + p^2U_2 + \dots \quad (A8)$$

Setting  $p = 1$ , results in the approximation to the solution of Eqn. (A8)

$$U = \lim_{p \rightarrow 1} V = U_0 + U_1 + U_2 + \dots \quad (A9)$$

The combination of the perturbation method and the homotopy method is called the homotopy perturbation method (HPM), which has eliminated limitations of the traditional perturbation techniques. The series Eqn. (A9) is convergent for more cases.

## Appendix B: Analytical solution Listeriosis linear Eqns. (1)-(4) using homotopy perturbation method (HPM).

$$\frac{dS_h}{dt} = \Omega_h + \omega R_l - \pi S_h - \mu_h S_h \quad (B1)$$

$$\frac{dI_l}{dt} = \pi S_h - (\delta + \mu_h + m) I_l \quad (B2)$$

$$\frac{dR_l}{dt} = \delta I_l - (\omega + \mu_h) R_l \quad (B3)$$

$$\frac{dC_p}{dt} = \rho I_l - \mu_b C_p \quad (B4)$$

Where,  $\Omega_h = 0.001$ ,  $\omega = 0.001$ ,  $\pi = 0.5$ ,  $\mu_h = 0.2$ ,  $\delta = 0.002$ ,  $m = 0.2$ ,  $\rho = 0.65$ ,  $\mu_b = 0.0025$ .

With the initial condition,  $\left(\frac{dS_h}{dt}, \frac{dI_l}{dt}, \frac{dR_l}{dt}, \frac{dC_p}{dt}\right) = \left(\frac{\Omega_h}{\mu_h}, 0, 0, 0\right)$  when  $t = 0$ ,

The initial conditions are

$$\frac{dS_h}{dt} = 0.005, \frac{dI_l}{dt} = 0, \frac{dR_l}{dt} = 0, \frac{dC_p}{dt} = 0 \quad (B5)$$

The homotopy from the Eqns. (B1)-(B4) can be constructed as follows:

$$(1-p) \left( \frac{dS_h}{dt} - \Omega_h + \pi S_h + \mu_h S_h \right) + p \left( \frac{dS_h}{dt} - \Omega_h - \omega R_l + \pi S_h + \mu_h S_h \right) = 0 \quad (B6)$$

where  $p$  is the embedding parameter and  $p \in [0,1]$ , The approximate solution of (B6) is

$$S = S_0 + pS_1 + p^2S_2 + \dots \quad (B7)$$

Substituting Eqns. (B6) into (B7), gives the following result.

$$\begin{aligned} & (1-p) \left( \frac{d}{dt} (S_0 + pS_1 + p^2S_2 + \dots) - \Omega_h + \pi(S_0 + pS_1 + p^2S_2 + \dots) + \mu_h(S_0 + pS_1 + p^2S_2 + \dots) \right) \\ & + p \left( \frac{d}{dt} (S_0 + pS_1 + p^2S_2 + \dots) - \Omega_h - \omega(R_0 + pR_1 + p^2R_2) + \pi(S_0 + pS_1 + p^2S_2 + \dots) \right. \\ & \left. + \mu_h(S_0 + pS_1 + p^2S_2 + \dots) \right) \\ & = 0 \end{aligned} \quad (B8)$$

$$S_h(0) = 0.003572e^{(-0.7t)} + 0.0014286 \quad (B9)$$

$$I_l(t) = 0.001776 - 0.00599e^{(-0.7t)} + 0.0042172e^{(-0.402t)} \quad (B10)$$

$$\begin{aligned} R_l(t) = & 0.0000177 - 0.0000419e^{(-0.402t)} + 0.0000241e^{(-0.7t)} + \\ & 0.0000027e^{(-0.201t)} \end{aligned} \quad (B11)$$

$$C_p(t) = 0.46176 - 0.006866e^{(-0.402t)} + 0.005592e^{(-0.7t)} - 0.4605e^{(-0.0025t)} \quad (B12)$$

## Appendix C (i) . Matlab program for the numerical solution of Listeriosis Model

```
function matrix1
options= odeset ('RelTol',1e-6,'Stats','on');
%initial conditions
Xo = [0.005,0,0,0];
tspan = [0,120];
tic
[t,X] = ode45(@TestFunction,tspan,Xo,options);
toc
figure
hold on
%plot(t, X(:,1),'-')
%plot(t, X(:,2),'-')
%plot(t, X(:,3),'-')
plot(t, X(:,4),'-')
legend('x1','x2','x3','x4')
ylabel('x')
xlabel('t')
return
function [dx_dt]= TestFunction(t,x)
a=0.001;b=0.001;c=0.5;d=0.2;e=0.002;f=0.2;g=0.65;p=0.0025;
dx_dt(1) = a+(b*x(3))-(c*x(1))-(d*x(1));
dx_dt(2) = (c*x(1))-((e+d+f)*x(2));
dx_dt(3) = (e*x(2))-((b+d)*x(3));
dx_dt(4) = (g*x(2))-(p*x(4));
dx_dt = dx_dt';
return
```

**Appendix C ( ii ) . Matlab program for the numerical solution of Anthrax Model**

```

function Anthrax
options= odeset ('RelTol',1e-6,'Stats','on');
%initial conditions
Xo = [0.001,0.001,0.001,1,2];
tspan = [0,120];
tic
[t,X] = ode45(@TestFunction,tspan,Xo,options);
toc
figure
hold on
%plot(t, X(:,1),'-')
%plot(t, X(:,2),'-')
%plot(t, X(:,3),'-')
%plot(t, X(:,4),'-')
plot(t, X(:,5),'-')
legend('x1','x2','x3','x4','x5')
ylabel('x')
xlabel('t')
return

```

```

function [dx_dt]= TestFunction(t,x)
a=0.001;b=0.02;c=0.01;d=0.2;e=0.05;f=0.33;g=0.2;h=0.005;p=0.0004;
dx_dt(1) = (a+(b*x(3))-(c*x(5)*x(1))-(d*x(1)));
dx_dt(2) = ((c*x(5)*x(1))-((f+d+g)*x(2)));
dx_dt(3) = ((f*x(2))-((b+d)*x(3)));
dx_dt(4) = (h-(e*x(2)*x(4))-(p*x(4)));
dx_dt(5) = ((e*x(2)*x(4))-(p*x(5)));
dx_dt = dx_dt';
return

```